Supporting Information

Yang et al. 10.1073/pnas.0914307107

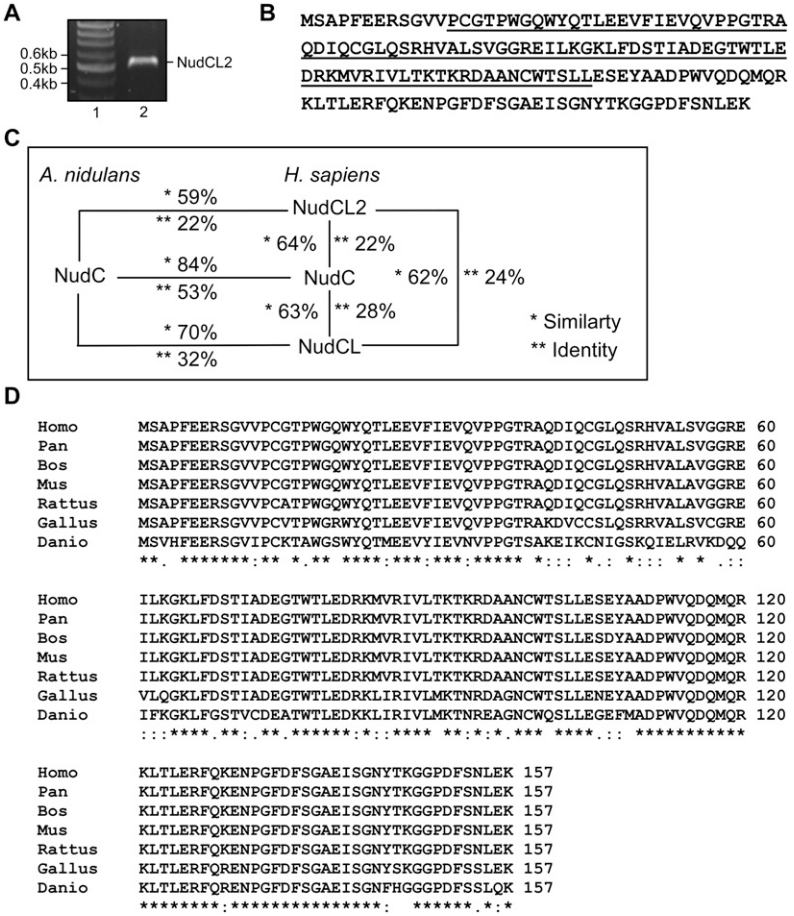

Fig. S1. Sequence analyses of NudCL2. (*A*) Molecular cloning of human NudCL2 gene. Human *NudCL2* was cloned by RT-PCR with total RNA extracted from HeLa cells (lane 2). Lane 1 is the molecular marker of DNA. (*B*) The deduced amino acid sequence of human NudCL2. The amino acid sequence of p23_NudC_like domain is underlined. (*C*) Similarity analysis of the members of NudC family in *A. nidulans* and *H. Sapiens*. (*D*) Comparison of putative NudCL2 orthologs in various species. The multiple alignment was generated using ClustalW program (http://www.ebi.ac.uk/Tools/clustalw2/index.html) with the sequences of NudCL2 orthologs from *Bos taurus* (Bos, ref: NP_001035643), *Gallus gallus* (Gallus, ref: XP_414494), *Pan troglodytes* (Pan, ref: XP_518082), *Mus musculus* (Mus, ref: NP_080299), *Rattus norvegicus* (Rattus, ref: NP_001009621), *Danio rerio* (Danio, ref: XP_001330930), and *Homo sapiens* (Homo, ref: NP_660309). *,the residues in that column are identical in all sequences in the alignment. : conserved substitutions have been observed. ., semiconserved substitutions are observed.

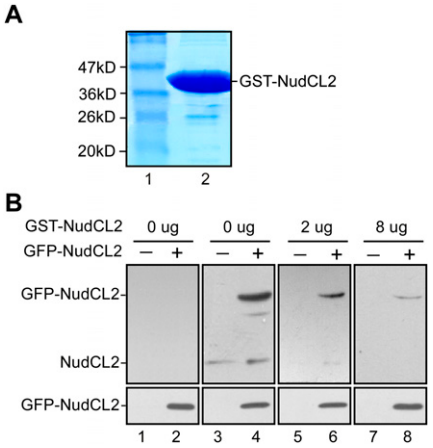

Fig. S2. Preparation of anti-NudCL2 antibody. (*A*) Purification of GST-fused NudCL2 protein (GST-NudCL2). Full-length human *NudCL2* cDNA was subcloned into pGEX-5×-1 (GST fusion vector). Recombinant GST-NudCL2 generated in *E. coli DH5α* were purified by incubation with glutathione-agarose beads followed by elution. Purified GST-NudCL2 was resolved by SDS/PAGE and subjected to Coomassie brilliant blue staining (lane 2). Lane 1 is a protein marker. (*B*) Characterization of anti-NudCL2 antibody. Rabbit polyclonal anti-NudCL2 antibody raised against GST-NudCL2 protein was affinity-purified. The extracts from HeLa cells transfected with either pGFP-NudCL2 or pGFP vector were subjected to Western analysis. The blots were incubated with preimmune serum or affinity-purified anti-NudCL2 antibody with different amounts of GST-NudCL2 (*Upper*). The blots were also probed with anti-GFP antibody (*Lower*).

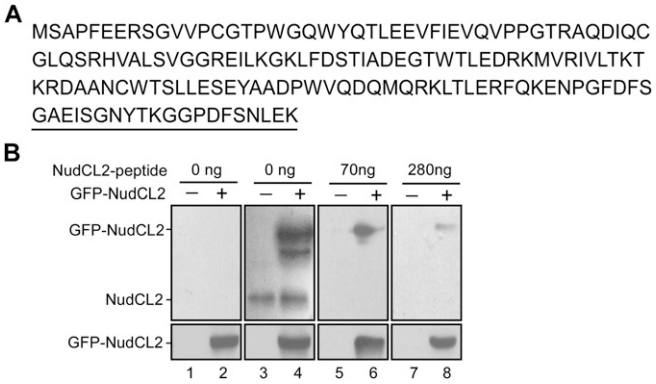

Fig. S3. Characterization of anti-NudCL2 peptide antibody (the antibody against a synthetic peptide of NudCL2). (*A*) The peptide sequence from human NudCL2 for antibody production is underlined. (*B*) Identification of anti-NudCL2 peptide antibody. Rabbit polyclonal anti-NudCL2 peptide antibody was generated by using the synthetic peptide of NudCL2 as antigen (Proteintech). The antibody was affinity-purified with the synthetic NudCL2 peptide. The extracts from HeLa cells transfected with pGFP-NudCL2 or pGFP vector were subjected to Western analysis. The blots were incubated with preimmune serum or anti-NudCL2 peptide antibody with various amounts of the synthetic NudCL2 peptide (*Upper*). The blots were also probed with anti-GFP antibody (*Lower*).

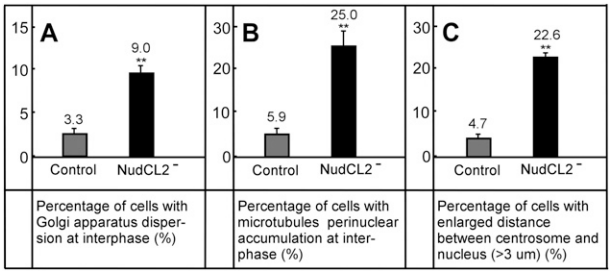

Fig. S4. The frequency of cellular phenotypes induced by depletion of NudCL2. HeLa cells were transfected with either pS-con or pS-NudCL2 and pBABE-puro. Puromycin was added to select the transfection-positive cells at 24 h after transfection. At 72 h posttransfection, the cells were subjected to immunofluorescence analyses with the indicated antibodies (Fig. 3). DNA was visualized by DAPI. The frequencies of cells with dispersion of Golgi apparatus (*A*), perinuclear microtubule enrichment (*B*) and enlarged distance between the centrosome and nucleus (*C*) were measured, respectively. Data are expressed as the mean ± SD of three independent experiments ($n > 200$, each). Significance determined by one-way ANOVA is expressed as: ** $P < 0.01$ versus control.

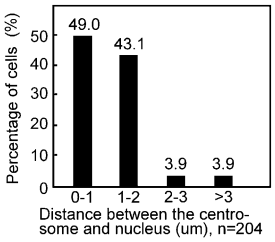

Fig. S5. The distance between the centrosome and nucleus in HeLa cells. HeLa cells grown on coverslips were subjected to immunofluorescence microscopy with anti-γ tubulin antibody. DNA was stained with DAPI. The distance between the centrosome and nucleus was defined as the shortest distance from the centrosome to the edge of nucleus. The cells with different distances between the centrosome and nucleus were counted.

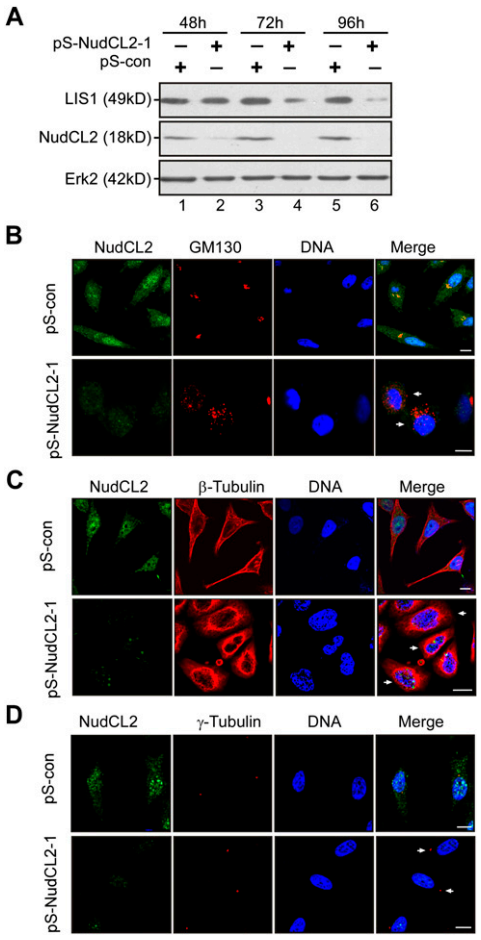

Fig. S6. Depletion of NudCL2 with pS-NudCL2-1 induces multiple cellular phenotypes. HeLa cells were transfected with either pS-con or pS-NudCL2-1 and pBABE-puro at the ratio of 7:1. The targeting sequence of pS-NudCL2-1 vector was 5′-agagagatgcagcaaattg-3′, corresponding to the region 277–295 relative to the first nucleotide of the start codon on *NudCL2*. At 24 h after transfection, puromycin was added to select the transfection-positive cells. (*A*) The cells were harvested at various times and subjected to immunoblotting analyses. (*B–D*) At 72 h posttransfection, the cells were analyzed by immunofluorescence experiments with the indicated antibodies. DNA was stained with DAPI. (Scale bar, 10 μm.) The cells indicated with arrows showed the dispersion of Golgi apparatus (*B*). The microtubule perinuclear enrichment was detected in cells with arrows (*C*). The cells with arrows exhibit a significant increase in the distance between the centrosome and nucleus (>3 μm) (*D*).

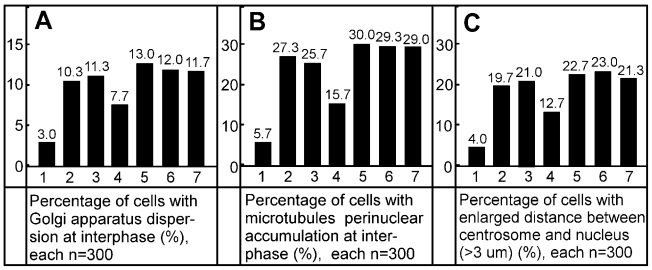

Fig. S7. Overexpression of LIS1 partially reverses the cellular phenotypes caused by NudCL2 depletion. HeLa cells were cotransfected with pBABE-puro and the following groups of plasmids. These groups are 1, pS-con; 2, pS-NudCL2; 3, pS-NudCL2 and pFLAG; 4, pS-NudCL2 and pFLAG-LIS1; 5, pS-LIS1; 6, pS-LIS1 and pFLAG; 7, pS-LIS1 and pFLAG-NudCL2, respectively. At 24 h after transfection, puromycin was added to enrich the transfection-positive cells. At 72 h posttransfection, the cells were subjected to immunofluorescence analysis with anti-NudCL2, GM130, and β and γ tubulin antibodies. DNA was stained with DAPI. The frequencies of cells with Golgi dispersion (*A*), perinuclear accumulation of microtubule (*B*), and enlarged distance between the centrosome and nucleus (>3 μm) (*C*) were determined, respectively. The data revealed that overexpression of LIS1 partially counteracted the phenotypes of NudCL2-depleted cells (group 4 compared with groups 2 and 3). However, ectopic expression of NudCL2 failed to reverse the cellular phenotypes caused by LIS1 knockdown (group 7 compared with groups 5 and 6).

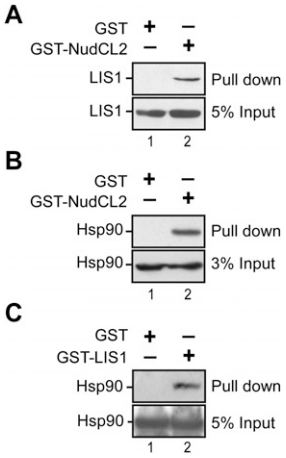

Fig. S8. The interaction among NudCL2, LIS1 and Hsp90 in vitro. (*A*–*B*) GST-NudCL2 associates with LIS1 and Hsp90 in vitro. Purified GST-NudCL2 was incubated with the lysates of HeLa cells. Either LIS1 (*A*) or Hsp90 (*B*) that interacts with GST-NudCL2 was detected by Western analysis using the indicated antibodies. (*C*) GST-LIS1 interacts with Hsp90 in vitro. Purified GST-LIS1 was incubated with the lysates of HeLa cells. Hsp90 that binds to GST-LIS1 was determined by immunoblotting with anti-Hsp90 antibody.

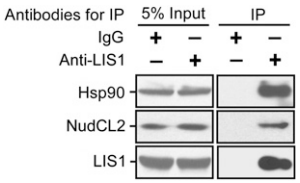

Fig. S9. Endogenous LIS1 binds to endogenous NudCL2 and Hsp90. Two aliquots of lysates from HeLa cells were subjected to immunoprecipitation experiments with either anti-mouse IgG or anti-LIS1 antibody, respectively. Immunoprecipitated proteins were analyzed by Western blotting with the indicated antibodies.

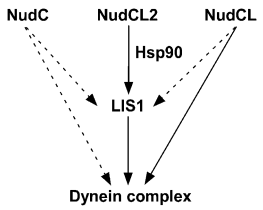

Fig. S10. A possible model for the regulation of the LIS1/dynein pathway by the NudC family in mammals. The black solid arrows show direct interactions with functional relevance. The interactions with unknown function are represented by dash arrow. The directions of arrows indicate the assumed direction of information transfer.